

# Spherical collapse and virialization in $f(T)$ gravities

Rui-Hui Lin,<sup>a</sup> Xiang-Hua Zhai,<sup>a</sup> Xin-Zhou Li<sup>a</sup>

<sup>a</sup>Shanghai United Center for Astrophysics (SUCA), Shanghai Normal University, 100 Guilin Road, Shanghai 200234, China

E-mail: [1000379711@smail.shnu.edu.cn](mailto:1000379711@smail.shnu.edu.cn), [zhaixh@shnu.edu.cn](mailto:zhaixh@shnu.edu.cn), [kychz@shnu.edu.cn](mailto:kychz@shnu.edu.cn)

**Abstract.** Using the classical top-hat profile, we study the non-linear growth of spherically symmetric density perturbation and structure formation in  $f(T)$  gravities. In particular, three concrete models, which have been tested against the observation of large-scale evolution and linear perturbation of the universe in the cosmological scenario, are investigated in this framework, covering both minimal and nonminimal coupling cases of  $f(T)$  gravities. Moreover, we consider the virialization of the overdense region in the models after they detach from the background expanding universe and turn around to collapse. We find that there are constraints in the magnitude and occurring epoch of the initial perturbation. The existence of these constraints indicates that a perturbation that is too weak or occurs too late will not be able to stop the expanding of the overdense region. The illustration of the evolution of the perturbation shows that in  $f(T)$  gravities, the initial perturbation within the constraints can eventually lead to clustering and form structure. The evolution also shows that nonminimal coupling models collapse slower than the minimal coupling one.

**Keywords:**  $f(T)$  theory; top-hat collapse; virialization

---

## Contents

<b>1</b>	<b>Introduction</b>	<b>1</b>
<b>2</b>	<b>From TEGR to <math>f(T)</math> models</b>	<b>2</b>
2.1	The field equations	2
2.2	Observationally tested models	4
<b>3</b>	<b>Spherical top-hat collapse</b>	<b>5</b>
<b>4</b>	<b>Virialization of the collapse</b>	<b>9</b>
<b>5</b>	<b>Conclusion and discussion</b>	<b>12</b>
<b>A</b>	<b>Roots of the principal quintic</b>	<b>17</b>

---

## 1 Introduction

At the end of the last century, the astronomical observation of high redshift type Ia supernovae (SNeIa) indicated that our universe is not only expanding, but also accelerating, which conflicts with our deepest intuition of gravity. Current observations, such as cosmic microwave background (CMB), baryon acoustic oscillations (BAO) and large scale structure (LSS), converge on the fact of accelerating expansion. In order to make reasonable sense of this acceleration, an exotic component of the universe, the mysterious dark energy (DE), has been introduced. Although many efforts have been made, the identity and physical nature of DE still seem to evade disclosure. Besides seeing DE as a real content of our universe, one possible way to address the problem is to modify gravitation theory such that the acceleration could be attributed to this modification (for review, see, e.g., [1]).

One of the extensively studied modified gravities is the  $f(R)$  gravity, in which one starts from the standard General relativity (GR), and extends the standard Hilbert-Einstein action to an arbitrary function of the Ricci scalar  $R$ [2, 3]. A further extension of  $f(R)$  gravity proposed in [4] and then studied in [4–7] is to consider the nonminimal coupling between matter and gravity, i.e. the  $f(R, \mathcal{L}_m)$  gravity, where  $\mathcal{L}_m$  is the Lagrangian density of matter. On the other hand, one can also modify the gravitation theory starting from the Teleparallel Equivalent of General Relativity (TEGR) [8–11]. In the Lagrangian of TEGR, the torsion scalar  $T$  takes the place of the Ricci scalar  $R$ , and hence in analogous to  $f(R)$ ,  $f(T)$ [12–14] and nonminimal coupling  $f(T, \mathcal{L}_m)$  gravities [15, 16] have been studied. Despite the equivalence between TEGR and GR,  $f(T)$  gravities are different from  $f(R)$  gravities. One of the important advantages of  $f(T)$  gravities is that the field equations are second order instead of fourth order. It is also noticed that non-trivial  $f(T)$  gravities violate the Lorentz invariance[17–19] and particular choices of tetrad are important to get viable models[20].

Concerning large scale evolution of the universe and the linear perturbations of the background,  $f(T)$  gravities have been compared with the cosmological observation data including CMB, BAO and SNeIa [12, 16, 21]. While the SNeIa data capture the late time accelerating behavior (redshift  $z < 3$ ), and the data of BAO and inhomogeneity of CMB

provide mostly the imprints of the early development and linear perturbations of the background before recombination ( $z > 1000 \sim 1500$ ), most structures such as stars, galaxies and clusters of galaxies are formed from the non-linear evolution of perturbations during the post-recombination epoch, which is usually referred as the Dark Ages ( $10 < z < 1000$ ). However, a fully relativistic treat of this non-linear perturbation is not currently available. Thus it is usually handled by  $N$ -body simulation (see e.g. [22–25]), which can be cumbersome and time-consuming, and is not practical for one to use to study different gravitation models. On the other hand, there has been intermediate approximations to the full-fledged theory before turning to simulation, one of which is spherical collapse model [26, 27]. In this simple semi-analytic model, a spherical overdense region evolves with the expanding background universe, and slows down and turns from expanding to collapsing. As a simple but fundamental tool to describe the growth of gravitationally bounded systems, this model has been used in various studies of gravitation theories in recent years [28–37]. The model has also been compared with the pseudo-Newtonian approach [38, 39] and it is found that the two approximation schemes convey identical equations for the density contrast.

After the turning around from expanding to collapsing, the overdense region shall virialize and be prevented from falling into a singularity. For gravitationally bounded systems, virialization is also a powerful approach with a long history. In fact, the discrepancy between the virial mass  $M_{\text{vir}}$  and the total baryonic mass  $M_b$  of a cluster contributed to the awareness of the existence of dark matter. However, the virial theorem depends on the gravitation theory, and hence the corresponding theorems in different modified gravities have drawn a lot of attention lately [40–45]. In the context of spherical collapse, virialization provides a more realistic picture of the collapsing structures, and enable ones to calculate the main features of them (collapse factor, virial density, virial mass, etc.), which may be useful in further analytic investigation or numerical simulation (e.g. NFW profile [46] to describe the  $N$ -body simulation).

In this paper, we look into the collapse of a spherically symmetric perturbation for models in  $f(T)$  gravities with a classical top-hat profile, including both minimal and nonminimal matter-gravity coupling cases. Moreover, we consider the virialization of the collapse after the turn-around point. The paper is organized as follows: in Section 2, we briefly review the bases and cosmologically tested models of the  $f(T)$  gravities, including both minimal and nonminimal matter-gravity coupling cases. In Sec.3, we consider the spherical top-hat collapse and evolution of perturbation in these models. We study the virialization of the collapse in Sec.4. Sec.5 contains our conclusions and discussions.

We are going to use the Latin letters ( $a, b, c, \dots = 0, 1, 2, 3$ ) to denote the tangent space indices, and Greek letters ( $\mu, \nu, \rho, \dots = 0, 1, 2, 3$ ) to denote the spacetime indices. We assume the Lorentz metric of Minkowski spacetime

$$\eta = \eta_{ab} dx^a \otimes dx^b \tag{1.1}$$

has the form  $\eta_{ab} = \text{diag}(+1, -1, -1, -1)$ . And we use the unit  $c = 1$  throughout the paper.

## 2 From TEGR to $f(T)$ models

### 2.1 The field equations

In the torsional formulations of gravity, one uses tetrad fields  $\{e_a, e^a\}$  as the fundamental dynamical variables. The tetrad fields form an orthonormal base of the tangent space  $T_p\mathcal{M}$

at each point  $p$  on the spacetime differentiable manifold  $\mathcal{M}$ . The spacetime metric  $g$

$$g = g_{\mu\nu} dx^\mu \otimes dx^\nu \quad (2.1)$$

is related to the tangent space metric  $\eta$  by

$$\eta_{ab} = g(e_a, e_b) = g_{\mu\nu} e_a^\mu e_b^\nu, \quad (2.2)$$

or conversely,

$$g_{\mu\nu} = \eta_{ab} e_\mu^a e_\nu^b. \quad (2.3)$$

And hence the determinant

$$|e| \equiv \det(e_\mu^a) = \sqrt{-g}. \quad (2.4)$$

One then can use the tetrad field to define the curvatureless Weitzenböck connection[47]

$$\tilde{\Gamma}_{\nu\mu}^\lambda \equiv e_a^\lambda \partial_\mu e_\nu^a = -e_\nu^a \partial_\mu e_a^\lambda \quad (2.5)$$

instead of the torsionless Levi-Civita one. The torsion and contorsion tensors are then given by

$$T_{\mu\nu}^\lambda \equiv \tilde{\Gamma}_{\nu\mu}^\lambda - \tilde{\Gamma}_{\mu\nu}^\lambda = e_i^\lambda (\partial_\mu e_\nu^i - \partial_\nu e_\mu^i), \quad (2.6)$$

and

$$K^{\mu\nu}{}_\rho \equiv -\frac{1}{2} (T^{\mu\nu}{}_\rho - T^{\nu\mu}{}_\rho - T_\rho^{\mu\nu}), \quad (2.7)$$

respectively. Utilizing the tensor

$$S_\rho^{\mu\nu} \equiv \frac{1}{2} (K^{\mu\nu}{}_\rho + \delta_\rho^\mu T^{\lambda\nu}{}_\lambda - \delta_\rho^\nu T^{\lambda\mu}{}_\lambda), \quad (2.8)$$

one can define the torsion scalar

$$T \equiv T^\rho{}_{\mu\nu} S_\rho^{\mu\nu}. \quad (2.9)$$

TEGR[9–11] uses this scalar  $T$  as the gravitation Lagrangian density. And the minimal matter-gravity coupling  $f(T)$  gravity extends it to an arbitrary function of  $T$ . The non-minimal coupling  $f(T)$  gravity[15] further extends the matter Lagrangian term  $\mathcal{L}_m$  into  $(1 + f_2(T))\mathcal{L}_m$ . To be unifiable, we write the action in the following form:

$$S = -\frac{1}{16\pi G} \int |e| (1 + f_1(T)) T d^4x + \int |e| (1 + f_2(T)) \mathcal{L}_m d^4x. \quad (2.10)$$

And the actions of TEGR and minimal coupling  $f(T)$  gravity correspond to the  $f_1, f_2 = 0$  and  $f_2 = 0$  cases of Eq.(2.10), respectively. With the action principle applied on Eq.(2.10) with respect to the tetrad field, the field equation is then given by

$$\frac{4}{|e|} f \partial_\beta (|e| S_\sigma^{\alpha\beta} e_a^\sigma) + 4e_a^\sigma S_\sigma^{\alpha\beta} \partial_\beta f + 4f S_\rho^{\alpha\sigma} T^\rho{}_{\sigma\beta} e_a^\beta + (1 + f_1) T e_a^\alpha = -16\pi G (1 + f_2) \mathcal{T}_\beta^\alpha e_a^\beta, \quad (2.11)$$

where  $f \equiv 1 + f_1(T) + f_1'(T)T - 16\pi G f_2'(T)\mathcal{L}_m$ , and  $\mathcal{T}_\beta^\alpha$  is the energy-momentum tensor of matter given by

$$\frac{\delta(|e|\mathcal{L}_m)}{\delta e_\alpha^a} = -|e| \mathcal{T}_\beta^\alpha e_a^\beta. \quad (2.12)$$

And it takes the usual form for perfect fluid

$$\mathcal{T}_{\mu\nu} = pg_{\mu\nu} - (\rho + p)u_\mu u_\nu, \quad (2.13)$$

where  $p$  and  $\rho$  are the pressure and energy density of the matter, respectively, and  $u^\mu$  is the 4-velocity.

The covariant derivative (related to the Levi-Civita connection) of Eq.(2.11) gives

$$\nabla^\nu \mathcal{T}_{\mu\nu} = -\frac{f_2'(T)\nabla^\nu T}{1 + f_2(T)}(\mathcal{T}_{\mu\nu} + g_{\mu\nu}\mathcal{L}_m). \quad (2.14)$$

This suggests that the energy-momentum tensor is no longer conservative. However, contracting Eq.(2.14) with  $u^\mu$ , we have

$$\begin{aligned} u^\mu \nabla^\nu \mathcal{T}_{\mu\nu} &= \frac{f_2'(T)\nabla^\nu T}{1 + f_2(T)}(\rho - \mathcal{L}_m) \\ &= -u^\mu \nabla_\mu \rho - (\rho + p)\nabla_\mu u^\mu. \end{aligned} \quad (2.15)$$

If we take the matter Lagrangian density to be  $\mathcal{L}_m = \rho$ [48–51], then in cosmological cases, as discussed in Ref.[16], Eq.(2.15) will return to the usual form of conservation law of matter in Friedmann-Lemaître-Robertson-Walker (FLRW) metric.

## 2.2 Observationally tested models

Consider a flat FLRW universe with metric in Cartesian coordinates

$$g_{\mu\nu} = \text{diag}(1, -a^2(t), -a^2(t), -a^2(t)), \quad (2.16)$$

with scale factor  $a(t)$ . It is found[20] that for this form of metric, the diagonal vierbein  $e^a_\mu = \text{diag}(1, a(t), a(t), a(t))$  is a viable choice for  $f(T)$  gravities. And then the torsion scalar  $T = -6H^2$ , where  $H = \dot{a}/a$  is the Hubble parameter, and the overdot denotes derivative with respect to time. The 00 entry of Eq.(2.11) then reads

$$12fH^2 - 6(1 + f_2)H^2 = 16\pi G(1 + f_2)\rho. \quad (2.17)$$

When  $f_1, f_2 = 0$ , i.e.  $f = 1$ , Eq.(2.17) gives the usual Friedmann's equation in GR or TEGR, and when  $f_2 = 0$ , Eq.(2.17) gives the field equation of minimal coupling  $f(T)$  gravities.

For another equation to determine the system, one can either use the rest components of Eq.(2.11) or the evolution of matter. Here we take the latter scheme. From Eq.(2.15), if we take  $\mathcal{L}_m = \rho$  and assume the matter is dust-like  $p \ll \rho$ , we can have the familiar evolution of matter  $\rho = \rho_0(a_0/a)^3$ , where  $\rho_0$  and  $a_0$  are the energy density of matter and scale factor at present time, respectively. Usually  $a_0$  is set to be 1.

In Ref.[16], we have constructed two concrete models of nonminimal coupling  $f(T)$  gravities for cosmological fitting. For completeness, here we consider one additional model of minimal coupling  $f(T)$  gravity. They are listed as follows:

- Model I:  $f_1 = \frac{12BH_0^4}{T^2}$ ,  $f_2 = 0$ ;
- Model II:  $f_1 = H_0(-T)^{-\frac{1}{2}}$ ,  $f_2 = \frac{-2AH_0^2}{\Omega_{m0}T}$ ;
- Model III:  $f_1 = \frac{12BH_0^4}{T^2}$ ,  $f_2 = \frac{-2AH_0^2}{\Omega_{m0}T}$ ,

where  $A, B$  are the parameters of the models,  $H_0$  is the Hubble parameter at present time and  $\Omega_{m0} = \frac{8\pi G\rho_0}{3H_0^2}$  is the matter density parameter. Model I represents the case of minimal coupling  $f(T)$  gravity, while Model II and III are the models of nonminimal coupling  $f(T)$  gravity constructed and fitted in Ref.[16]. Then Eq.(2.17) can be unifiably written as

$$\left(\frac{\dot{a}}{a}\right)^2 = \Omega_{m0}H_0^2a^{-3} + \frac{(B + Aa^{-3})H_0^4}{\left(\frac{\dot{a}}{a}\right)^2}. \quad (2.18)$$

Denoting  $E = H/H_0$ , we have

$$E^2 = \Omega_{m0}a^{-3} + Aa^{-3}E^{-2} + BE^{-2} \quad (2.19)$$

with  $1 = \Omega_{m0} + A + B$ . Model I, II, III correspond to the cases  $A = 0, B = 0$  and  $A, B \neq 0$ , respectively.

We use the data set of SNeIa, BAO and CMB, the same as Ref.[16], to find the best-fit values of parameters for Model I, and retain the fitting results of Model II and III, listed in Table 1.

**Table 1.** Best-fit parameters for the models

parameters	models		
	Model I	Model II	Model III
$\Omega_{m0}$	$0.274 \pm 0.008$	$0.367 \pm 0.011$	$0.302 \pm 0.011$
$H_0$	$73.73 \pm 0.79$	$60.97 \pm 0.44$	$68.54 \pm 1.27$
$A$	-	$0.633 \pm 0.011$	$0.188 \pm 0.048$
$\chi_{\min}^2/\text{d.o.f.}$	707.455/739	729.429/739	683.846/739

### 3 Spherical top-hat collapse

The classical spherical top-hat collapsing formalism considers a spherical region with uniformly perturbed energy density immersed in the homogeneous universe. The initial magnitude of the perturbation is denoted as  $\delta_i$ , and it occurs at the redshift  $z_i$ , where the subscript "i" hereinafter indicates the initial evaluation of the quantities at this very moment. The initial radius of the overdense region and the density of the universe are denoted as  $R_i$  and  $\rho_i$ , respectively. Thus the initial density of the overdense region is  $\rho_i(1 + \delta_i)$  and the scale factor at that time is  $a_i = 1/(1 + z_i)$ .

This region then detaches from the rest of the universe and evolves on its own like a non-spatial-flat universe [26–28, 39]. For this reason, we need the equation of a spatial curved universe besides the flat background evolution. For a universe with spatial curvature  $k$ , the torsional formalism gives the torsion scalar[20]

$$T = -6H^2 + \frac{6k}{a^2}. \quad (3.1)$$

And the 00 entry of Eq.(2.11) is

$$(2f - 1 - f_1) \left(6H^2 - \frac{6k}{a^2}\right) = 16\pi G(1 + f_2)\rho. \quad (3.2)$$

When  $k = 0$ , Eq.(2.17) is recovered. For the three models listed above, Eq.(3.2) is then

$$\left(\frac{\dot{a}}{a}\right)^2 - \frac{k}{a^2} = \Omega_{\text{m}0} H_0^2 a^{-3} + \frac{(B + Aa^{-3}) H_0^4}{\left(\frac{\dot{a}}{a}\right)^2 - \frac{k}{a^2}}. \quad (3.3)$$

Denoting  $H_i = H(a_i)$ ,  $\tilde{k} = \frac{k}{a_i^2 H_i^2}$ ,  $\Omega_{\text{mi}} = \frac{8\pi G \rho_0}{3H_i^2 a_i^3}$ ,  $\tilde{A} = A \frac{H_0^4}{a_i^3 H_i^4}$  and  $\tilde{B} = B \frac{H_0^4}{H_i^4}$ , we have

$$\left(\frac{\dot{a}}{H_i a_i}\right)^2 - \tilde{k} = \Omega_{\text{mi}} \frac{a_i}{a} + \frac{\tilde{A} \left(\frac{a}{a_i}\right) + \tilde{B} \left(\frac{a}{a_i}\right)^4}{\left(\frac{\dot{a}}{H_i a_i}\right)^2 - \tilde{k}}. \quad (3.4)$$

This is the equation governing the scale factor  $a$  in a spatial curved universe. Therefore the equation for the radius  $R$  of the overdense region is in the similar form,

$$\left(\frac{\dot{R}}{h_i R_i}\right)^2 - \tilde{k} = \Omega_{\text{mi}} (1 + \delta_i) \frac{R_i}{R} + \frac{\tilde{A} \left(\frac{R}{R_i}\right) + \tilde{B} \left(\frac{R}{R_i}\right)^4}{\left(\frac{\dot{R}}{h_i R_i}\right)^2 - \tilde{k}}, \quad (3.5)$$

with

$$1 - \tilde{k} = \Omega_{\text{mi}} (1 + \delta_i) + \frac{\tilde{A} + \tilde{B}}{1 - \tilde{k}}, \quad (3.6)$$

where  $h = \dot{R}/R$  is the expansion rate of the region and initially  $h_i = H_i$ .

As the evolution continues, the region may stop expanding and start collapsing due to the overdensity. At the turn-around point, if it ever occurs, the radius of the region reaches its maximum  $R_{\text{max}}$  and  $\dot{R} = 0$ . Denoting  $\beta \equiv R_{\text{max}}/R_i$ , we can rewrite Eq.(3.5) at the turn-around point as

$$\tilde{B}\beta^5 + \tilde{A}\beta^2 - \tilde{k}^2\beta - \tilde{k}\Omega_{\text{mi}}(1 + \delta_i) = 0. \quad (3.7)$$

It is a quintic equation of  $\beta$ . The region will turn from expanding to collapsing if only Eq.(3.7) has real positive root(s). According to the Passare-Tsikh solution[52] of the principal quintic

$$mx^5 + nx^2 + x + 1 = 0, \quad (3.8)$$

Eq.(3.7) has real positive root(s) if and only if (See Appendix A)

$$3125|m|^2 - 256|m| + 108|n|^5 - 27|n|^4 + 625|m||n| - 2250|n|^2|m| < 0 \quad (3.9)$$

where

$$m = -\frac{\tilde{B}\Omega_{\text{mi}}^4(1 + \delta_i)^4}{\tilde{k}^6}, \quad n = -\frac{\tilde{A}\Omega_{\text{mi}}(1 + \delta_i)}{\tilde{k}^3}. \quad (3.10)$$

For Model I ( $A = 0$ ), the quadratic term of Eq.(3.8) vanishes, while the discriminant (3.9) is still valid and reduces to  $3125|m| - 256 < 0$ , namely

$$\frac{(1 + z_i)^{12} (1 + \delta_i)^3}{H_i^{12} \tilde{k}^6} < \frac{256}{3125 B G^4 H_0^{12} \Omega_{\text{m}0}^4}. \quad (3.11)$$

For Model II ( $B = 0$ ), the quintic term of Eq.(3.8) vanishes and the equation reduces to a quadratic one. And Eq.(3.9) gives the same inequality as the discriminant of the quadratic:  $4|n| - 1 < 0$ , namely

$$-\frac{(1 + z_i)^3 (1 + \delta_i)}{H_i^2 \tilde{k}^3} < \frac{1}{4A\Omega_{\text{m}0} H_0^2}. \quad (3.12)$$

For Model III ( $A, B \neq 0$ ), similar inequality can be obtained, which is omitted here for its lengthiness. In Eqs.(3.11), (3.12) and the corresponding inequality for Model III,  $H_i$  and  $\tilde{k}$  depend on  $z_i$  and  $\delta_i$  according to Eqs.(2.19) and (3.6), respectively. And thus for given  $A$  and  $B$ , these inequalities give constraints on the time ( $z_i$ ) and magnitude ( $\delta_i$ ) of the initial perturbation. For the three models listed above, we have plotted these constraints in Fig.1, where the models have taken the best-fit parameters listed in Table 1. Any pairs of ( $z_i, \delta_i$ ) above the illustrated lines can guarantee real positive root(s) of Eq.(3.7), namely make sure that the overdense region will eventually collapse and form structure. The result is not surprising in that a perturbation that either is too weak (low  $\delta_i$ ) or occurs too late (low  $z_i$ , and such that the matter of the universe is too thin) will not be able to provide a self-gravity strong enough to slow down the expanding and turn the region into collapsing. Compared to the minimal coupling Model I, the constraint for Model II is more stringent, while the one for Model III is slightly looser.

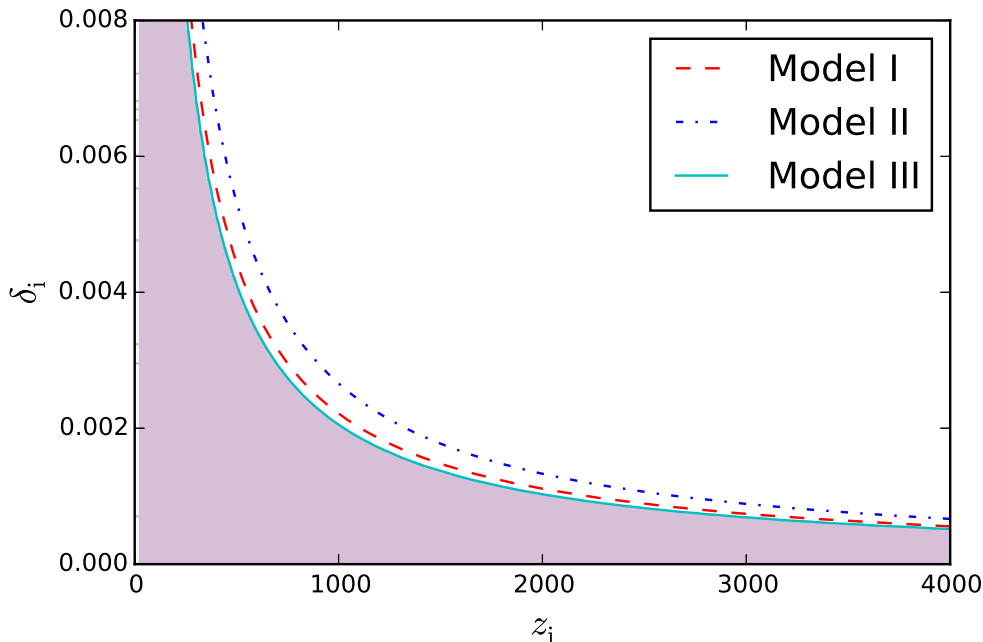


**Figure 1.** The constraints of  $z_i$  and  $\delta_i$  for Model I(dashed), II(dashdot) and III(solid), where the models have taken the best-fit parameters listed in Table 1. The shaded area is forbidden for not being able to turn the region from expanding to collapsing.

Note that if  $\tilde{A} = \tilde{B} = 0$  in Eq.(3.7),  $\beta = -\Omega_i(1 + \delta_i)/\tilde{k} > 0$  is automatically the physical root we need. That is, for Einstein-de Sitter universe in GR or TEGR, as shown in many standard cosmology textbooks, these constraints for  $\delta_i$  and  $z_i$  do not exist and collapse will always happen eventually due to the lack of persistent driving source of the expansion.

For a given model and initial perturbation, Eq.(3.5) determines the evolution of the radius of the overdense region, which can be carried out numerically. The evolution of  $R/R_i$  of all three models are plotted in Fig.2, where we have set  $z_i = 1200$ ,  $\delta_i = 0.003$ , and taken the best-fit parameters from Table 1. The variation of  $\delta_i$  will also alter the evolution of  $R/R_i$ , which is illustrated in Fig.3 for Model III.



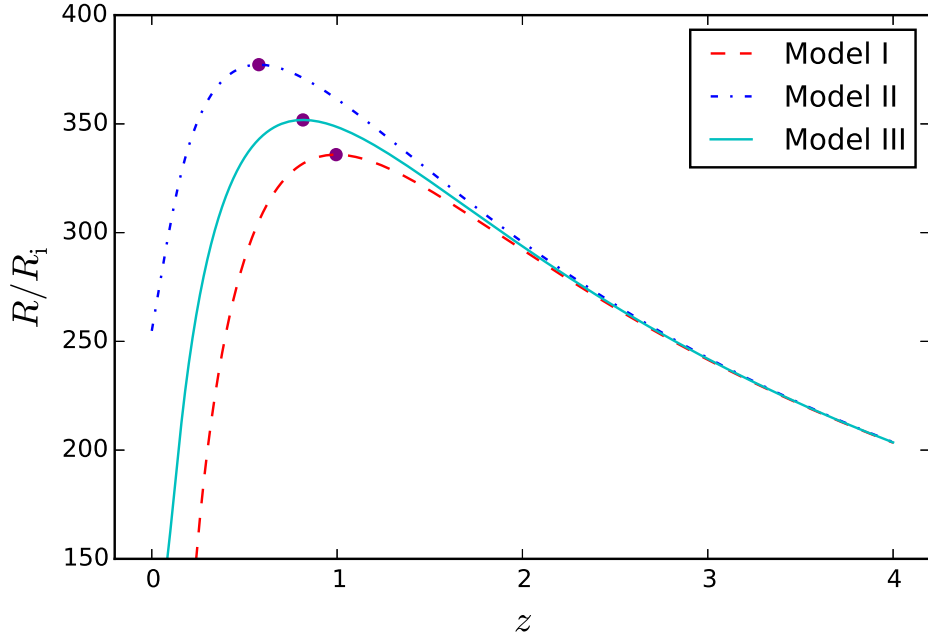


**Figure 2.** The evolution of  $R/R_i$  of all three models, where  $z_i = 1200$ ,  $\delta_i = 0.003$ , and the models have taken the best-fit parameters from Table 1.

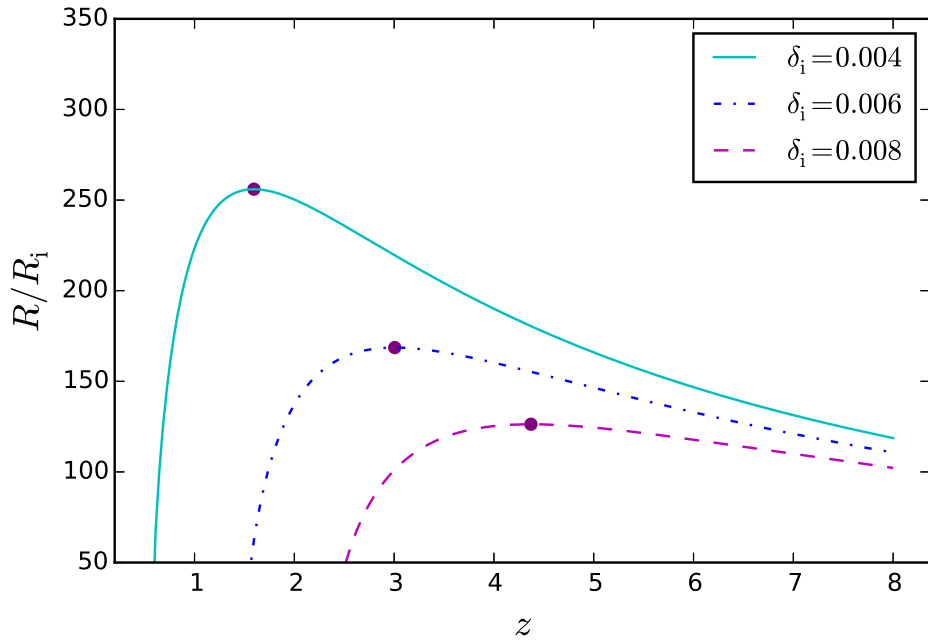


**Figure 3.** The evolution of  $R/R_i$  for different  $\delta_i$  in model III, where  $z_i = 1200$ , and the models have taken the best-fit parameters from Table 1.

We have also calculated the evolutions of the expansion rate  $h = \dot{R}/R$  of the region, and plotted them in Fig.4. The markers in Figs.2-4 correspond to the turn-around points of the models, the evaluations of which are listed in Table 2. One can see that compared to the minimal coupling model (Model I), the collapsing processes are slower in the nonminimal coupling models (Model II and III), thus the turn-arounds happen at lower redshift  $z_{\text{ta}}$  and consequently larger  $\beta = R_{\text{max}}/R_i$  are reached. In the case of Model II where effective dark energy is entirely attributed to the nonminimal torsion-matter coupling, the collapsing is the slowest among the three, and largest  $\beta$  is reached at latest time  $z_{\text{ta}}$ .

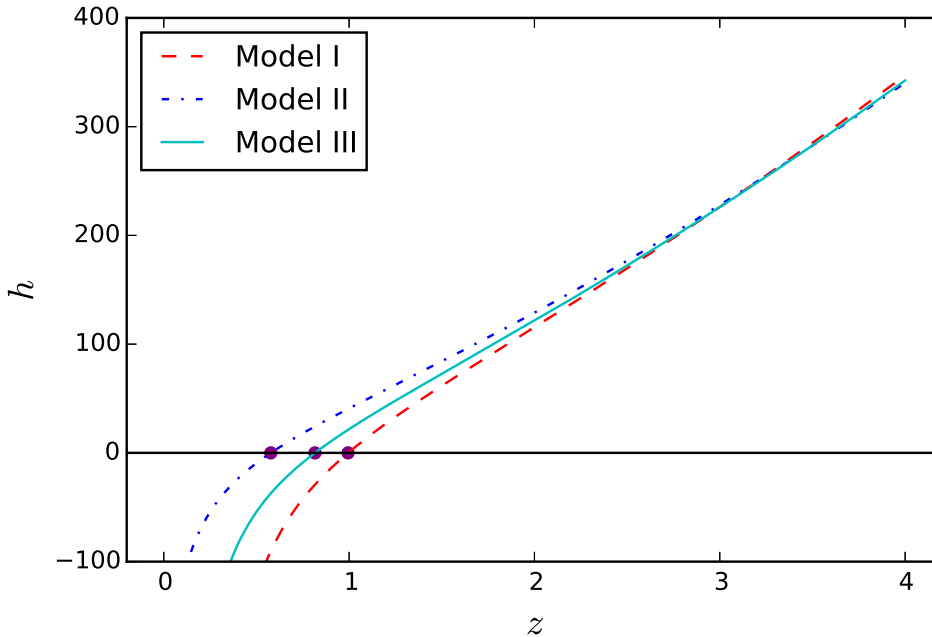


**Figure 4.** The evolution of  $h = \dot{R}/R$  of all three models, where  $z_i = 1200$ ,  $\delta_i = 0.003$ , and the models have taken the best-fit parameters from Table 1.

Moreover, it is also worth considering the evolution of the density contrast between the collapsing region and the background universe. Denoting the density of the universe as  $\rho_u = \rho_i(a_i/a)^3$  and that of the collapsing region as  $\rho_c = \rho_i(1 + \delta_i)(R_i/R)^3$ , one then can define the density contrast  $\Delta$  by  $\rho_c = \rho_u \Delta$ . Utilizing the evolutions of  $R$  from Eq.(3.5) and  $a$  from Eq.(2.18), we have carried out the evolution of  $\Delta$ , and illustrated in Fig.5.

#### 4 Virialization of the collapse

In Fig.5, one can see that after the turn-around point, the region governed by Eq.(3.5) will soon collapse into a singularity, which, however, is not the actual fate for all the collapsing structures. As the clustering continues, the kinetic energy of the matter will be no longer negligible, which will eventually take the system to an equilibrium and stop the collapsing. This highly non-linear process is simplified and described by the virialization of a self-gravity system.

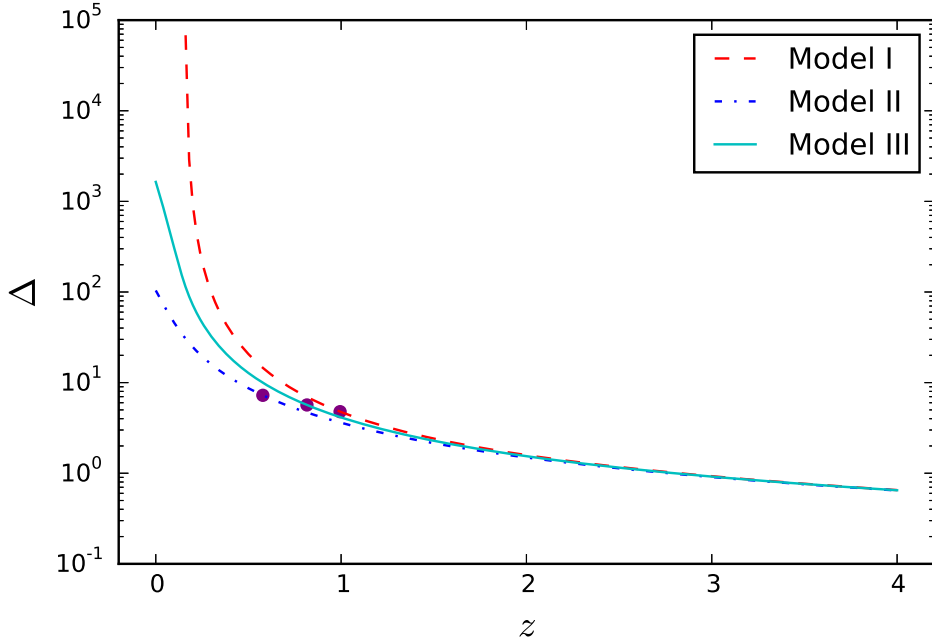


**Figure 5.** The evolution of  $\Delta = \rho_c/\rho_u$  of all three models, where  $z_i = 1200$ ,  $\delta_i = 0.003$ , and the models have taken the best-fit parameters from Table 1.

The relativistic virial theorem starts from the Boltzmann's equation for collisionless particles (see, e.g., [53, 54]):

$$u^\mu \partial_\mu F_B + \frac{dp^\mu}{d\tau} \frac{\partial F_B}{\partial p^\mu} = 0, \quad (4.1)$$

where  $u^\mu$  is the 4-velocity,  $p^\mu$  is the 4-momentum,  $dp^\mu/d\tau$  is the 4-force, and  $F_B$  is the Boltzmann distribution function on the 6-dimensional phase space  $\{\vec{x}, \vec{p}\}$ . Assume that  $F_B$  vanishes sufficiently rapidly as the velocities tend to infinity, Eq.(4.1) will lead to the virial theorem (see, e.g., [26, 40, 45]):

$$2\mathcal{E}_K + \int \vec{f} \cdot \vec{x} dV = 0, \quad (4.2)$$

where  $\mathcal{E}_K$  is the kinetic energy of the system and  $\vec{f}$  is the force that the system imposes on the local volume element  $dV$  located at  $\vec{x}$ . The integral is taken over the whole system.

Usually, the force  $\vec{f}$  or the 4-force  $dp^\mu/d\tau$  should be obtained from the geodesic equation, or the non-geodesic equation for the nonminimal coupling cases (see, e.g. [15, 16, 51]), but that requires full knowledge of the spherical symmetric solution to the field equation of the modified gravity, which we do not currently have. On the other hand, the Newtonian-like gravity force and potential are connected to the cosmology. In GR, this argument is originated by Milne[55], and presented in many standard cosmology textbooks.

Consider a comoving test particle located at  $r = r_i a/a_i = r_0 a$ , where  $r_0 = r_i/a_i$  is its

comoving position, then Eq.(2.18) can be written in terms of  $r$  as

$$\begin{aligned} \left(\frac{\dot{r}}{r}\right)^2 &= \frac{8\pi G}{3} \frac{\rho_0 r_i^3}{a_i^3 r^3} + \frac{AH_0^4 r_i^3}{a_i^3 r^3} \left(\frac{r}{\dot{r}}\right)^2 + BH_0^4 \left(\frac{r}{\dot{r}}\right)^2 \\ &= \frac{8\pi G \rho_i}{3} \left(\frac{r_i}{r}\right)^3 + \left[\tilde{A} \left(\frac{r_i}{r}\right)^3 + \tilde{B}\right] h_i^4 \left(\frac{r}{\dot{r}}\right)^2, \end{aligned} \quad (4.3)$$

which is the equation of motion of the test particle. Denoting the mass inside a spherical region of radius  $r$  as  $m = 4\pi r_i^3 \rho_i / 3$ , we have

$$\frac{(\dot{r})^2}{2} = \frac{Gm}{2r} + \frac{1}{2} \sqrt{\left(\frac{Gm}{r}\right)^2 + h_i^4 (\tilde{A} r_i^3 r + \tilde{B} r^4)}. \quad (4.4)$$

In classic analogy,  $\dot{r}$  is the velocity of the particle, and the left hand side of Eq.(4.4),  $(\dot{r})/2$ , is the kinetic energy density of it. We then can identify the right hand side of Eq.(4.4) as the gravitational potential per unit mass at  $r$

$$V(r) = -\frac{Gm}{2r} - \frac{1}{2} \sqrt{\left(\frac{Gm}{r}\right)^2 + h_i^4 (\tilde{A} r_i^3 r + \tilde{B} r^4)}, \quad (4.5)$$

where  $m = 4\pi r_i^3 \rho_i / 3 = 4\pi r^3 \rho / 3$ . When  $\tilde{A} = \tilde{B} = 0$ , it is obviously the Newtonian potential.

And the force per unit mass acting on the volume element at  $r$  is

$$\begin{aligned} f(r) &= -\frac{dV(r)}{dr} \\ &= -\frac{Gm}{2r^2} + \frac{-2\frac{G^2 m^2}{r^3} + h_i^4 (4\tilde{B} r^3 + \tilde{A} r_i^3)}{4\sqrt{\frac{G^2 m^2}{r^2} + h_i^4 (\tilde{B} r^4 + \tilde{A} r_i^3 r)}}. \end{aligned} \quad (4.6)$$

Hence the virial theorem is

$$\begin{aligned} 2\mathcal{E}_K &= -\int_0^R f(r) r 4\pi r^2 \rho dr \\ &= -\frac{9M}{20R} \frac{h_i^4 R^3 (2\tilde{B} R^3 + \tilde{A} R_i^3)}{\sqrt{G^2 M^2 + h_i^4 R^3 (\tilde{B} R^3 + \tilde{A} R_i^3)}} \\ &\quad + \frac{3GM^2}{10R} + \frac{3M}{10R} \sqrt{G^2 M^2 + h_i^4 R^3 (\tilde{A} R_i^3 + \tilde{B} R^3)}. \end{aligned} \quad (4.7)$$

From Eq.(4.5), if a spherical system has a radius  $R$  and mass  $M = 4\pi R^3 \rho / 3$ , the total potential energy of it is

$$\begin{aligned} V_{\text{tot}}(R) &= \int_0^R V(r) 4\pi r^2 \rho dr \\ &= -\frac{3GM^2}{10R} - \frac{3M}{10R} \sqrt{G^2 M^2 + h_i^4 R^3 (\tilde{A} R_i^3 + \tilde{B} R^3)}, \end{aligned} \quad (4.8)$$

where  $R_i^3 = R^3 \rho / \rho_i$ .

Although usually the energy conservation is considered violated in the nonminimal coupling cases due to the extra force and non-geodesic movement (see Eq.(2.14) or, e.g., [15, 16, 51]), here the energy conservation is still hold in form during the collapse, since we have put the effect of the extra force into the gravitation potential. And hence, we have

$$\mathcal{E}_{\text{K,vir}} + V_{\text{tot}}(R_{\text{vir}}) = V_{\text{tot}}(R_{\text{max}}), \quad (4.9)$$

where  $R_{\text{vir}}$  is the radius of the collapsing region when it reaches virialization.

Denote  $\alpha = R_{\text{vir}}/R_i$ , Eq.(4.9) gives

$$\begin{aligned} & \frac{\Omega_{\text{mi}}(1 + \delta_i)}{2\beta} + \frac{1}{\beta} \sqrt{\frac{\Omega_{\text{mi}}^2(1 + \delta_i)^2}{4} + \beta^3(\tilde{A} + \tilde{B}\beta^3)} \\ = & \frac{\Omega_{\text{mi}}(1 + \delta_i)}{4\alpha} + \frac{1}{2\alpha} \sqrt{\frac{\Omega_{\text{mi}}^2(1 + \delta_i)^2}{4} + \alpha^3(\tilde{A} + \tilde{B}\alpha^3)} \\ & + \frac{3\alpha^2(2\tilde{B}\alpha^2 + \tilde{A})}{4\sqrt{\frac{\Omega_{\text{mi}}^2(1 + \delta_i)^2}{4} + \alpha^3(\tilde{A} + \tilde{B}\alpha^3)}}, \end{aligned} \quad (4.10)$$

where  $\beta = R_{\text{max}}/R_i$ . Using the numerical evaluation of  $\beta$  from Eq.(3.7) and  $\alpha$  from Eq.(4.10), one can obtain the collapse factor  $\lambda = R_{\text{vir}}/R_{\text{max}} = \alpha/\beta$ . Furthermore, one can in turn calculate the redshifts and density contrasts at turn-around ( $z_{\text{ta}}, \Delta_{\text{ta}}$ ) and virialization ( $z_{\text{vir}}, \Delta_{\text{vir}}$ ) from the evolutions plotted in Figs.2 and 5. The evaluations at the turn-around and virialization for the models with  $z_i = 1200$ ,  $\delta_i = 0.003$  are listed in Table 2. The corresponding results for Einstein de Sitter universe are also listed for comparison. One can see that the results for the minimal coupling model (Model I) are relatively closer to the E-dS model, while the nonminimal coupling models (Model II and III) virialize slower. The virialization for Model II even happens in the future ( $z_{\text{vir}} < 0$ ) for the given setting.

**Table 2.** Turn-around and virialization of the models

	models			
	Model I	Model II	Model III	E-dS
$z_{\text{ta}}$	0.994	0.578	0.816	1.031
$R_{\text{max}}/R_i$	335.864	377.229	351.814	334.333
$\Delta_{\text{ta}}$	5.781	8.242	6.666	5.551
$z_{\text{vir}}$	0.258	-0.189	0.110	0.363
$R_{\text{vir}}/R_i$	167.245	176.837	171.118	167.167
$\Delta_{\text{vir}}$	186.470	589.284	253.331	146.841
$\lambda$	0.498	0.469	0.486	0.5

## 5 Conclusion and discussion

Most structures in our universe such as stars, galaxies and clusters of galaxies are formed from the nonlinear evolution of perturbations during the post-recombination epoch. Ideally, we should hope to investigate the problem by combining  $f(T)$  models of large-scale structure formation with hydrodynamic codes which follow the dynamical and thermal histories of the diffuse intergalactic gas. A fully relativistic treat of this non-linear perturbation is not

currently available. The intrinsically non-linear nature of the processes is usually handled by N-body simulation, which can be cumbersome and time-consuming, and is not practical for one to use to study different gravitation models. However, the spherical top-hat profile is the simplest analytic model which can be used to study the non-linear growth of spherically symmetric density perturbation and structure formation in  $f(T)$  gravities. Though density perturbation will not be spherically symmetric in most of the realistic cases, the spherical top-hat profile can give significant enlightenment for the true picture of physics. Anyhow, the top-hat profile is a useful means for the non-linear evolution of perturbation. In this paper, we have studied the non-linear growth of perturbation in  $f(T)$  gravities, including both minimal and nonminimal coupling cases. And then we looked into the virialization of the collapsing region after the turn-around point. Our main results are as follows:

- (i) The numerical calculation of redshift  $z_{\text{ta}}$  at the turn-around point indicates incontrovertibly that galaxies and other large-structure features must have formed relatively late in the history of the universe in three  $f(T)$  models. If we take appropriate initial conditions  $\delta_i$  at  $z = z_i$ , the value of  $z_{\text{ta}}$  will not conflict with the late time formation of the structures (see Fig.3). As a matter of fact, the population of galaxies and quasars have evolved dramatically over the redshift range  $0 < z < 6$ .
- (ii) The perturbations were still in the linear regime at  $z \sim 1000$ , but as they entered upon the later phase of the post-recombination era, their evolution became non-linear. In Ref.[16], we have given the relation between  $a(t)$  and  $t$  at the post-recombination era for the  $f(T)$  cosmological models (see Eqs. (45)-(47) in Ref.[16]). Thereby, we can use the linear evolution equation of density perturbation and get the result of  $\delta(z_{\text{ta}})$  which is far more smaller than that of top-hat profile. By the time the perturbed sphere had stopped expanding, its density in the three models is already 5.781, 8.242 and 6.666 times greater than that of the background density. These pictures are consistent with the primitive spherical top-hat collapse (E-dS model).
- (iii) The existence of turn-around point is the crux of matter in the non-linear collapse of density perturbations. The perturbation can always reaches maximum radius for the primitive top-hat model. There are constraints of initial value  $\delta_i$  at  $z_i$  in three  $f(T)$  models (see Fig.1), which reinforce our intuition that in an accelerating expanding universe, a magnitude of perturbation  $\delta_i$  that is too weak will not be able to turn the overdense region from expanding to collapsing. In Ref. [16], we have given  $z_{\text{crit}} = 0.3298$  and  $0.6694$  for Model II and Model III, respectively. Here,  $z_{\text{crit}}$  is defined as the critical values of the redshift through which the universe changes to the acceleration phase from the deceleration one. Therefore, we have a reasonable explanation for our numerical results. We find that compared to Model III, the collapsing processes are slower since  $z_{\text{crit}}$  is smaller in Model II (see Fig.2). Furthermore, the turn-around happens at lower redshift  $z_{\text{ta}}$  and consequently larger  $R_{\text{max}}/R_i$  is reached.
- (iv) Outwardly, the subsequent collapse occurs very rapidly (see Fig. 2) after the redshift of  $z_{\text{ta}}$  and the spherical perturbed region collapses ultimately to a black hole. In reality, however, it is much more likely to form some sort of bound object. If the density becomes high enough, we cannot neglect the internal pressure in the overdense region. As the gas cloud collapses, its temperature increases until pressure gradients becomes sufficient to balance the attractive force of gravitation. The ultimate result is a system

which satisfies the virial theorem. By the numerical calculation, we have obtained the density contrast between the collapsing region and the background universe by the time the region is virialized (see Table 2). Since the critical value  $z_{\text{crit}}$  of Model II is smaller than that of Model III, we have a good reason to expound the slower virialized process for Model II.

- (v) The numerical results show that nonminimal coupling models collapse slower than the minimal coupling model, which may be an indication for alleviating the small scale problems [56, 57].
- (vi) The virialization for Model II happens in the future ( $z_{\text{vir}} = -0.189$ ) for the given setting  $z_i = 1200$  and  $\delta_i = 0.003$ . This is not strange because the spherical top-hat collapse is a highly idealised picture. The better approximation is to assume that the collapsing regions are ellipsoidal with three unequal principal axes. In this model, the ellipsoid collapses to a 'pancake' which is the collapsing result of the non-linear regime in the more general case.

To sum up, the spherical top-hat collapse is a qualitative analysis which successfully expounds the aspects of non-linear evolution in  $f(T)$  gravities. But this is a highly idealised description, so we do not really expect that it is quantitatively consistent with the process of formation of bound structures in the expanding universe. For example, the observation of CMB requires  $\Delta T/T \sim 10^{-5}$ , which is corresponding to  $\delta\rho/\rho \sim 10^{-5}$  at  $z = 1200$ . In other words, the spherical top-hat collapse is only a toy model. For comparison with the observation, we should study further the pancake model and N-body simulations in  $f(T)$  gravities. We will look into these issues in the future works.

## References

- [1] S. Capozziello and M. De Laurentis, *Extended theories of gravity*, *Phys. Rep.* **509** (2011) 167–321.
- [2] T. P. Sotiriou and V. Faraoni, *f(R) theories of gravity*, *Rev. Mod. Phys.* **82** (2010) 451–497.
- [3] A. De Felice and S. Tsujikawa, *f(R) theories*, *Living Rev. Relativity* **13** (2010) 3.
- [4] O. Bertolami, C. G. Böhrmer, T. Harko and F. S. N. Lobo, *Extra force in f(R) modified theories of gravity*, *Phys. Rev. D* **75** (2007) 104016.
- [5] T. Harko, *Modified gravity with arbitrary coupling between matter and geometry*, *Phys. Lett. B* **669** (2008) 376–379.
- [6] T. Harko and F. S. N. Lobo, *f(R,  $\mathcal{L}_m$ ) gravity*, *Eur. Phys. J. C* **70** (2010) 373–379.
- [7] O. Bertolami and J. Páramos, *Mimicking dark matter through a non-minimal gravitational coupling with matter*, *J. Cosmol. Astropart. Phys.* **03** (2010) 009.
- [8] A. Einstein, *Riemannian geometry with maintaining the notion of distant parallelism*, *Sitzungsber. Preuss. Akad. Wiss. Phys. Math. Kl.* (1928) 217.
- [9] K. Hayashi and T. Shirafuji, *New general relativity*, *Phys. Rev. D* **19** (1979) 3524.
- [10] R. Aldrovandi and J. Pereira, *Teleparallel Gravity: An Introduction*. Fundamental Theories of Physics. Springer Netherlands, 2012, [10.1007/978-94-007-5143-9](https://doi.org/10.1007/978-94-007-5143-9).
- [11] J. W. Maluf, *The teleparallel equivalent of general relativity*, *Ann. Phys. (Berlin)* **525** (2013) 339–357.

- [12] G. R. Bengochea and R. Ferraro, *Dark torsion as the cosmic speed-up*, *Phys. Rev. D* **79** (2009) 124019.
- [13] E. V. Linder, *Einstein's other gravity and the acceleration of the universe*, *Phys. Rev. D* **81** (2010) 127301.
- [14] Y.-F. Cai, S. Capozziello, M. De Laurentis and E. N. Saridakis,  *$f(T)$  teleparallel gravity and cosmology*, *Rep. Prog. Phys.* **79** (2016) 106901.
- [15] T. Harko, F. S. N. Lobo, G. Otalora and E. N. Saridakis, *Nonminimal torsion-matter coupling extension of  $f(T)$  gravity*, *Phys. Rev. D* **89** (2014) 124036.
- [16] C.-J. Feng, F.-F. Ge, X.-Z. Li, R.-H. Lin and X.-H. Zhai, *Towards realistic  $f(T)$  models with nonminimal torsion-matter coupling extension*, *Phys. Rev. D* **92** (2015) 104038.
- [17] B. Li, T. P. Sotiriou and J. D. Barrow,  *$f(T)$  gravity and local lorentz invariance*, *Phys. Rev. D* **83** (2011) 064035.
- [18] T. P. Sotiriou, B. Li and J. D. Barrow, *Generalizations of teleparallel gravity and local lorentz symmetry*, *Phys. Rev. D* **83** (2011) 104030.
- [19] S. Bahamonde, C. G. Böhmmer and M. Wright, *Modified teleparallel theories of gravity*, *Phys. Rev. D* **92** (2015) 104042.
- [20] N. Tamanini and C. G. Böhmmer, *Good and bad tetrads in  $f(T)$  gravity*, *Phys. Rev. D* **86** (2012) 044009.
- [21] R. C. Nunes, S. Pan and E. N. Saridakis, *New observational constraints on  $f(T)$  gravity from cosmic chronometers*, *J. Cosmol. Astropart. Phys.* **08** (2016) 011.
- [22] A. Macciò, C. Quercellini, R. Mainini, L. Amendola and S. Bonometto, *Coupled dark energy: Parameter constraints from  $N$ -body simulations*, *Phys. Rev. D* **69** (2004) 123516.
- [23] N. Aghanim, A. C. da Silva and N. J. Nunes, *Cluster scaling relations from cosmological hydrodynamic simulations in a dark-energy dominated universe*, *Astron. Astrophys.* **496** (2009) 637–644.
- [24] M. Baldi, V. Pettorino, G. Robbers and V. Springel, *Hydrodynamical  $N$ -body simulations of coupled dark energy cosmologies*, *Mon. Not. R. Astron. Soc.* **403** (2010) 1684–1702.
- [25] B. Li, D. F. Mota and J. D. Barrow,  *$N$ -body simulations for extended quintessence models*, *Astrophys. J.* **728** (2011) 109.
- [26] J. E. Gunn and I. Gott, J. Richard, *On the infall of matter into clusters of galaxies and some effects on their evolution*, *Astrophys. J.* **176** (1972) 1.
- [27] T. Padmanabhan, *Structure formation in the universe*. Cambridge ; New York : Cambridge University Press, 1993.
- [28] D. F. Mota and C. van de Bruck, *On the spherical collapse model in dark energy cosmologies*, *Astron. Astrophys.* **421** (2004) 71–81.
- [29] I. Maor and O. Lahav, *On virialization with dark energy*, *J. Cosmol. Astropart. Phys.* **07** (2005) 003.
- [30] N. J. Nunes and D. F. Mota, *Structure formation in inhomogeneous dark energy models*, *Mon. Not. R. Astron. Soc.* **368** (2006) 751–758.
- [31] S. Basilakos, J. C. B. Sanchez and L. Perivolaropoulos, *Spherical collapse model and cluster formation beyond the  $\Lambda$  cosmology: Indications for a clustered dark energy?*, *Phys. Rev. D* **80** (2009) 043530.
- [32] S. Basilakos, M. Plionis and J. Solà, *Spherical collapse model in time varying vacuum cosmologies*, *Phys. Rev. D* **82** (2010) 083512.



- [33] P. Brax, R. Rosenfeld and D. Steer, *Spherical collapse in chameleon models*, *J. Cosmol. Astropart. Phys.* **08** (2010) 033.
- [34] R. A. A. Fernandes, J. P. M. de Carvalho, A. Y. Kamenshchik, U. Moschella and A. da Silva, *Spherical “top-hat” collapse in general-chaplygin-gas-dominated universes*, *Phys. Rev. D* **85** (2012) 083501.
- [35] E. Bellini, N. Bartolo and S. Matarrese, *Spherical collapse in covariant galileon theory*, *J. Cosmol. Astropart. Phys.* **06** (2012) 019.
- [36] W. Li and L. Xu, *Spherical top-hat collapse of a viscous unified dark fluid*, *Eur. Phys. J. C* **74** (2014) 2870.
- [37] T. R. P. Caramês, J. C. Fabris and H. E. S. Velten, *Spherical collapse for unified dark matter models*, *Phys. Rev. D* **89** (2014) 083533.
- [38] L. R. Abramo, R. C. Batista, L. Liberato and R. Rosenfeld, *Structure formation in the presence of dark energy perturbations*, *J. Cosmol. Astropart. Phys.* **11** (2007) 012.
- [39] L. R. Abramo, R. C. Batista, L. Liberato and R. Rosenfeld, *Physical approximations for the nonlinear evolution of perturbations in inhomogeneous dark energy scenarios*, *Phys. Rev. D* **79** (2009) 023516.
- [40] C. G. Böhmer, T. Harko and F. S. N. Lobo, *The generalized virial theorem in  $f(R)$  gravity*, *J. Cosmol. Astropart. Phys.* **03** (2008) 024.
- [41] A. S. Sefiedgar, K. Atazadeh and H. R. Sepangi, *Generalized virial theorem in palatini  $f(\mathcal{R})$  gravity*, *Phys. Rev. D* **80** (2009) 064010.
- [42] S. Capozziello, T. Harko, T. S. Koivisto, F. S. Lobo and G. J. Olmo, *The virial theorem and the dark matter problem in hybrid metric-palatini gravity*, *J. Cosmol. Astropart. Phys.* **07** (2013) 024.
- [43] M. Milgrom, *General virial theorem for modified-gravity mond*, *Phys. Rev. D* **89** (2014) 024016.
- [44] N. S. Santos and J. Santos, *The virial theorem in eddington-born-infeld gravity*, *J. Cosmol. Astropart. Phys.* **2015** (2015) 002.
- [45] R. Javadinezhad, J. T. Firouzjaee and R. Mansouri, *Relativistic virial relation for cosmological structures*, *Phys. Rev. D* **93** (2016) 023007.
- [46] J. F. Navarro, C. S. Frenk and S. D. M. White, *A universal density profile from hierarchical clustering*, *Astrophys. J.* **490** (1997) 493.
- [47] R. Weitzenböck, *Invarianten-Theorie*. P. Noordhoff, 1923.
- [48] Ø. Grøn and S. Hervik, *Einstein’s General Theory of Relativity: With Modern Applications in Cosmology*. Springer New York, 2007, [10.1007/978-0-387-69200-5](https://doi.org/10.1007/978-0-387-69200-5).
- [49] O. Bertolami, F. S. N. Lobo and J. Páramos, *Nonminimal coupling of perfect fluids to curvature*, *Phys. Rev. D* **78** (2008) 064036.
- [50] O. Minazzoli and T. Harko, *New derivation of the lagrangian of a perfect fluid with a barotropic equation of state*, *Phys. Rev. D* **86** (2012) 087502.
- [51] T. Harko, F. S. Lobo, G. Otalora and E. N. Saridakis,  *$f(T, \mathcal{T})$  gravity and cosmology*, *J. Cosmol. Astropart. Phys.* **12** (2014) 021.
- [52] M. Passare and A. Tsikh, *The Legacy of Niels Henrik Abel*, ch. Algebraic Equations and Hypergeometric Series, pp. 653–672. Springer Science, 2004.
- [53] J. C. Jackson, *The dynamics of clusters of galaxies in universes with non-zero cosmological constant, and the virial theorem mass discrepancy*, *Mon. Not. R. Astron. Soc.* **148** (1970) 249–260.

- [54] F. Debbasch and W. van Leeuwen, *General relativistic boltzmann equation, II: Manifestly covariant treatment*, *Physica A* **388** (2009) 1818–1834.
- [55] E. A. Milne, *A newtonian expanding universe*, *Q. J. Math.* **os-5** (1934) 64–72.
- [56] B. Moore, *Evidence against dissipation-less dark matter from observations of galaxy haloes*, *Nature* **370** (1994) 629–631.
- [57] M. Boylan-Kolchin, J. S. Bullock and M. Kaplinghat, *The milky way’s bright satellites as an apparent failure of  $\lambda$ cdm*, *Mon. Not. R. Astron. Soc.* **422** (2012) 1203–1218.

## A Roots of the principal quintic

As is known to all, a quintic equation does not have a general expression of roots. However, for principal quintic

$$mx^5 + nx^2 + x + 1 = 0, \quad (\text{A.1})$$

Passare and Tsikh[52] found that a root can be expressed as a series expansion:

$$x_5 = - \sum_{j,k \geq 0} \frac{(2j + 5k)!}{j!k!(j + 4k + 1)!} n^j (-m)^k, \quad (\text{A.2})$$

with the domain of convergence given by the condition

$$\begin{aligned} 3125|m|^2 - 4^4|m| + 2^23^3|n|^5 - 3^3|n|^4 + 25^2|m||n| \\ - 2 \cdot 3^25^3|n|^2|m| < 0. \end{aligned} \quad (\text{A.3})$$

Eq.(3.7) can be written in the form of Eq.(A.1) with

$$x = \frac{\tilde{k}\beta}{\Omega_{\text{mi}}(1 + \delta_{\text{i}})}, \quad (\text{A.4})$$

and

$$m = -\frac{\tilde{B}\Omega_{\text{mi}}^4(1 + \delta_{\text{i}})^4}{k^6}, \quad n = -\frac{\tilde{A}\Omega_{\text{mi}}(1 + \delta_{\text{i}})}{k^3}. \quad (\text{A.5})$$

For  $\tilde{A}, \tilde{B} > 0$  and  $\tilde{k} < 0$ , we have  $m < 0$  and  $n > 0$ . And then Eq.(A.2), if converges, gives a negative real root  $x_5 < 0$ . Since  $\tilde{k} < 0$ , Eq.(A.4) then gives a corresponding positive real root of Eq.(3.7) denoted as  $\beta_5 > 0$ . Thus, Eq.(A.3) with Eq.(A.5) gives a sufficient condition for Eq.(3.7) to have real positive root(s).

As for the necessity of Eq.(3.9), we know that Eq.(A.1) will have at least one real root, denoted as  $x_1$ . And  $x_1 > 0$  because  $m < 0$ . Since the derivative of Eq.(A.1),  $5mx^4 + 2nx + 1 = 0$ , only has two real roots, the quintic function  $mx^5 + nx^2 + x + 1$  has only two extrema. So the principal quintic equation (A.1) has at most three real roots. That is, Eq.(A.1) has a real root and a pair of conjugate complex roots for sure. This guaranteed pair of conjugate complex roots are denoted as  $x_2, x_3$ . Now  $x_5$  is either real (when Eq.(A.2) converges) or complex (when Eq.(A.2) diverges) depending on  $m, n$ , therefore it will not be one of the three roots  $x_1, x_2, x_3$ . Assume that the condition Eq.(A.3) is falsified and hence Eq.(A.2) diverges and  $x_5$  is complex. According to Vieta’s relation among the roots, the last root  $x_4 = -(x_1 + x_2 + x_3 + x_5)$ . Since  $x_2, x_3$  are conjugate complex roots and  $x_5$  is complex,  $x_4$  is complex, too. In other word, if Eq.(A.3) is falsified, Eq.(A.1) will have only one real root, and it is positive, and hence Eq.(3.7) will not have any real positive root. Thus, Eq.(3.9) is the necessary and sufficient condition for Eq.(3.7) to have real positive root(s).